Magnetocaloric response of Fe 75 Nb 10 B 15 powders partially amorphized by ball milling

J. J. Ipus, J. S. Blázquez, V. Franco, A. Conde, and L. F. Kiss

Citation: Journal of Applied Physics **105**, 123922 (2009); doi: 10.1063/1.3155982
View online: http://dx.doi.org/10.1063/1.3155982
View Table of Contents: http://scitation.aip.org/content/aip/journal/jap/105/12?ver=pdfcov
Published by the AIP Publishing

Magnetocaloric response of $Fe_{75}Nb_{10}B_{15}$ powders partially amorphized by ball milling

J. J. Ipus,[1] J. S. Blázquez,[1,a)] V. Franco,[1] A. Conde,[1,b)] and L. F. Kiss[2]
[1]*Dpto. Física de la Materia Condensada, ICMSE-CSIC, Universidad de Sevilla, P.O. Box 1065, 41080 Sevilla, Spain*
[2]*Research Institute for Solid State Physics and Optics, Hungarian Academy of Sciences, P.O. Box 49, 1525 Budapest, Hungary*

(Received 5 November 2008; accepted 25 May 2009; published online 29 June 2009)

The magnetocaloric response of mechanically alloyed $Fe_{75}Nb_{10}B_{15}$ powders was studied for samples with different amorphous and nanocrystal volume fractions. Thermomagnetic properties scale following a Ω^3 law for different milling processes, where Ω is the milling frequency. Curie temperature of the amorphous phase increases as the amorphous fraction increases due to its progressive enrichment in B. The peak magnetic entropy change, $|\Delta S_M^{pk}|$, as well as the refrigerant capacity increase with increasing amorphous fraction. The field dependence of $|\Delta S_M^{pk}|$ can be explained by the multiphase character of the studied samples. © *2009 American Institute of Physics*. [DOI: 10.1063/1.3155982]

I. INTRODUCTION

The magnetocaloric effect (MCE), i.e., the temperature change in magnetic materials due to a varying magnetic field, has been intensively studied in the past years.[1–3] Magnetic materials with a large MCE close to room temperature have attracted considerable attention due to their potential use in magnetic refrigeration, which is an environment friendly cooling technology and more energetically efficient than conventional gas compression-expansion refrigeration. In order to enhance the magnetocaloric response, materials with a big magnetic moment and a strong temperature dependence of magnetization close to the working temperature are needed.

MCE is inherent to any magnetic material, classified into two types: those presenting a first order magnetostructural transition and those presenting a second order magnetic transition. For the first type, giant MCE has been observed in intermetallic compounds of GdSiGe close to room temperature.[4–7] However, the presence of hysteresis is a drawback. In materials with a second order phase transition, this problem can be overcome but MCE is generally lower, Gd being the material used in refrigerator prototypes nowadays.[1,8]

Recently, the suitability of transition metal based alloys with second order magnetic transition[9–11] has been studied. For these alloys, the intensity of the magnetic entropy change peak is not higher than that of first order phase transition materials but MCE peaks are broader, which allows for an increased refrigerant capacity. In the case of Fe based amorphous alloys, the easiness for modifying the temperature of magnetic transition with compositional changes, their extremely reduced magnetic hysteresis, their enhanced electrical resistivity (which would reduce eddy current losses), and their lower cost are all beneficial characteristics for their application as magnetic refrigerants.

Most materials reported in the literature are bulk and only some works report on the MCE of powder alloys.[12–16] Powder materials can be easily obtained by mechanical alloying, which is a useful and versatile technique to produce metastable microstructures (amorphous, nanocrystalline, supersaturated solid solutions, etc) from elemental powders or alloys.[17]

Nanocrystalline alloys, whose MCE is not largely studied in the literature,[9,15,16,18] can be obtained by different ways: either by controlled crystallization of an amorphous precursor or by mechanical alloying. In this work, the magnetocaloric response of mechanically alloyed $Fe_{75}Nb_{10}B_{15}$ composition has been studied as a function of the ratio between crystalline and amorphous fractions.

II. EXPERIMENTAL

Partially amorphous $Fe_{75}Nb_{10}B_{15}$ alloy was produced by mechanical alloying from pure powders in a planetary ball mill Fritsch Pulverisette 4 Vario. The manipulation of the powder was done under argon atmosphere in a Saffron glove box. Details of the milling parameters can be found elsewhere.[19] Two different milling frequencies Ω were used in the aim of studying the applicability of the predicted Ω^3 law for the power release during milling.[20] In this way, results can be represented as a function of an equivalent time defined as $t_{eq}=(\Omega/150)^3 t$, where Ω is the milling frequency (in rpm units) and t is the experimental time. The milling process was limited to $t_{eq} \leq 508$ h in order to avoid a big increase in impurities in the alloy (e.g., Cr contamination from milling media affects the magnetic properties[21]). For the studied samples energy dispersive x-ray spectroscopy (Incax-sight of Oxford Instruments) shows a Cr content below 2 at. %. The temperature of the magnetic measurements

a)Electronic mail: jsebas@us.es.
b)Author to whom correspondence should be addressed. Tel.: (34)-95-455-28-85. FAX: (34)-95-461-20-97. Electronic mail: conde@us.es.

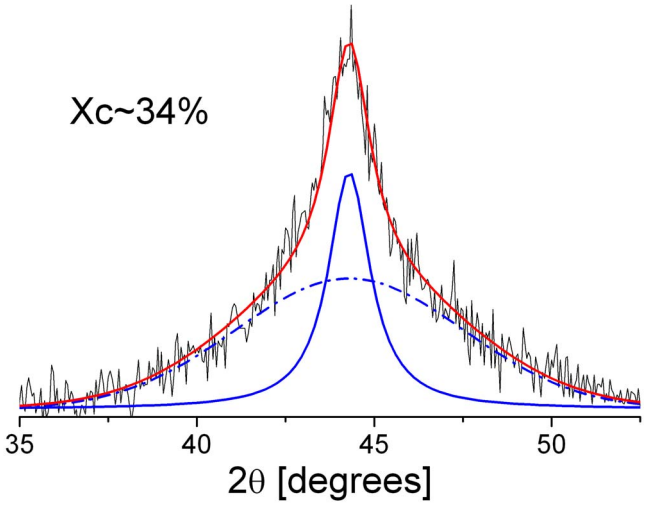

FIG. 1. (Color online) XRD pattern of a sample milled 300 h at 150 rpm showing the deconvolution of crystalline and amorphous contributions.

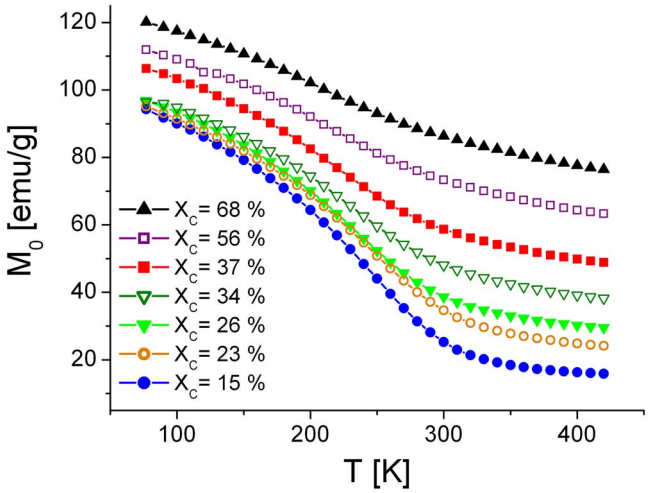

FIG. 2. (Color online) Temperature dependence of spontaneous magnetization for different crystalline volume fractions. Hollow symbols correspond to 150 rpm and solid symbols correspond to 350 rpm.

was kept well below crystallization temperature,[19] which ensures the microstructural stability of the samples.

Microstructure was studied from x-ray diffraction (XRD) using Cu $K\alpha$ radiation in a Bruker D8I diffractometer. Three phases were detected in the milled powder: nanocrystals of a bcc Fe(Nb,B) supersaturated solid solution, an amorphous matrix, and almost pure B inclusions.[19,22] The crystalline fraction was calculated from the area ratio between two contributions used to deconvolute the (110) diffraction peak (a Lorentzian contribution for the crystalline phase and a Gaussian one for amorphous phase). An example is given in Fig. 1.

The field dependence of magnetization was measured using a Lakeshore 7407 vibrating sample magnetometer using a maximum applied field $H=15$ kOe with a field step of 250 Oe at constant temperatures in the range of 77–420 K with increments of 10 K.

The magnetic entropy change due to the application of a magnetic field H has been evaluated by processing the temperature and field dependent magnetization curves using a numerical approach to the equation

$$\Delta S_M = \int_0^{H_{\max}} \left(\frac{\partial M}{\partial T}\right)_H dH, \tag{1}$$

where ΔS_M is the magnetic entropy change, M is the magnetization, and T is the temperature. The partial derivative is replaced by finite differences and the integration is performed numerically from zero field to a maximum value $H_{\max}$.

The refrigerant capacity can be defined in two ways: as the product of the peak entropy change times the full width at half maximum of the peak, RC_{FWHM}, and using the Wood and Potter method,[23] which corresponds to the maximum area of the rectangle under the ΔS_M curve, RC_{WP}. Superconducting quantum interference device (SQUID) magnetometer (Quantum Design MPMS-5S) was used to check the saturation magnetization at 5 K and magnetocaloric response at 5 T for selected samples.

III. RESULTS

Figure 2 shows the spontaneous magnetization M_0 as a function of temperature for all studied samples. M_0 was obtained as the extrapolation to zero field of a linear fitting of the high field magnetization. As the amorphous fraction increases, a reduction in M_0 is observed. Moreover, the change in magnetization at the Curie transition ascribed to the amorphous phase developed during milling[19] (~250 K, measured using the inflection point method) becomes more evident. Hence the magnetization at low temperatures corresponds to both amorphous and α-Fe(Nb,B) phases, whereas at high temperatures, it corresponds to the α-Fe(Nb,B) nanocrystals.

Figure 3 shows the temperature dependence of magnetic entropy change for a maximum applied magnetic field of 15 kOe for different crystalline fractions. It can be observed that the magnitude of the peak increases with increasing amorphous fraction, as the ferro-paramagnetic transition of the amorphous phase is the main responsible for the MCE in the explored temperature range. Moreover, there is a displace-

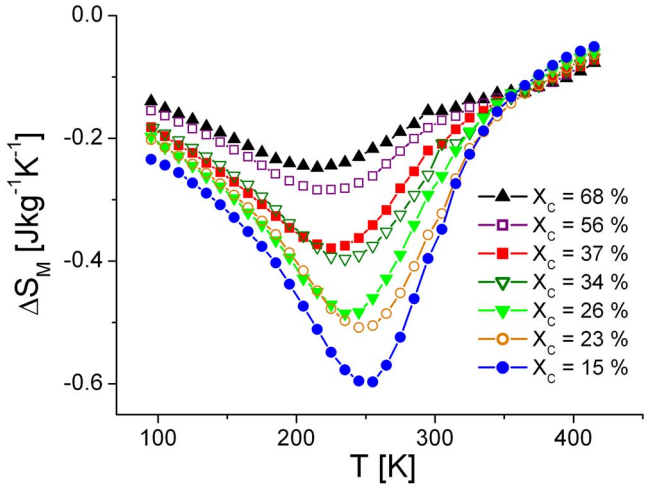

FIG. 3. (Color online) Magnetic entropy change curves as a function of crystalline fraction for a maximum applied field of 15 kOe. Hollow symbols correspond to 150 rpm and solid symbols correspond to 350 rpm.

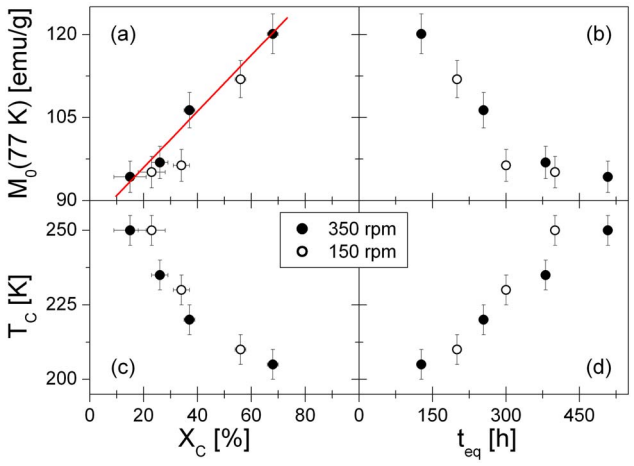

FIG. 4. (Color online) [(a) and (b)] Crystalline fraction and equivalent milling time dependence of spontaneous magnetization at 77 K, respectively, and [(c) and (d)] Curie temperature of the amorphous phase, respectively. Hollow symbols correspond to 150 rpm and solid symbols correspond to 350 rpm Line in (a) corresponds to linear fitting of the data.

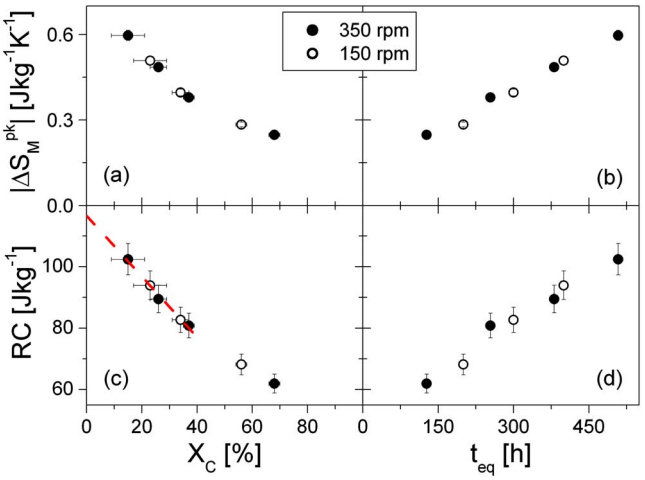

FIG. 5. (Color online) [(a) and (b)] Crystalline fraction and equivalent milling time dependence of magnetic entropy change at peak temperature, respectively, and [(c) and (d)] refrigerant capacity, respectively. Hollow symbols correspond to 150 rpm and solid symbols correspond to 350 rpm. Line in (c) corresponds to linear fitting of the data for $X_C < 50\%$.

ment in the peak to higher temperatures with the increase in the amorphous fraction, well correlated with the evolution in the Curie temperature. The entropy change at high temperatures follows the opposite trend than that observed at the peak (decreases with increasing the amorphous fraction), in agreement with the sum rule expected for two phase systems.[24]

IV. DISCUSSION

Figures 4(a) and 4(b) show the magnetization at the lowest measured temperature, $M_0(77\ \mathrm{K})$, as a function of crystalline fraction and equivalent milling time, respectively. The latter plot confirms that the evolution of this magnitude rescales following the Ω^3 law predicted for different milling processes.[20] An approximately linear relationship between $M_0(77\ \mathrm{K})$ and crystalline fraction is observed, which can be understood using a very simple model described by

$$M_0(77\ \mathrm{K}) = \langle M_0^C \rangle X_C + \langle M_0^A \rangle (1 - X_C),$$

where $\langle M_0^C \rangle$ and $\langle M_0^A \rangle$ are the average saturation magnetizations of the crystalline and amorphous phases, respectively. Averages should be used because the composition of both crystalline and amorphous phases is expected to change along the milling process. From linear fitting of Fig. 4(a) data, the values $\langle M_0^C \rangle = 134 \pm 10$ emu/g and $\langle M_0^A \rangle = 84 \pm 3$ emu/g have been determined. Values obtained from SQUID measurements at 5 K yield a similar value for $\langle M_0^C \rangle = 136 \pm 6$ emu/g and a higher value for $\langle M_0^A \rangle = 96 \pm 1$ emu/g, in agreement with the lower Curie temperature for the amorphous phase. The value of $\langle M_0^A \rangle$ is of the same order as those reported for Fe–X–B (X=Zr, Nb, Mo, etc.) amorphous alloys.[25,26] However, the spontaneous magnetization value found for $\langle M_0^C \rangle$ is smaller than that of pure Fe,[27] which should be ascribed to the presence of Nb, B, and Cr in the remaining crystalline phase as well as to the nanometric size of the crystals.

Figure 4(c) shows the Curie temperature T_C of the amorphous phase against crystalline fraction. It can be observed that, as amorphous fraction increases, the Curie temperature increases. This enhancement can be explained by a progressive increase in boron content of the amorphous phase with the milling time. In fact, the ferromagnetism is intimately related to the average Fe–Fe interatomic distances and an increase in such distances due to interstitial B atoms favors ferromagnetism via the reinforcement of the exchange coupling and the density of states.[28,29] In the present studied alloy, the mixing of B with the other elements is not completed even after 400 h at 150 rpm.[22] At this stage, remaining B inclusions (~50 nm in size) were still observed, although with a smaller size than that found for 50 h milling (100–200 nm). It could be necessary to assume an increase of ~3 at. % B into the amorphous matrix to explain the observed increase of T_C from X_C=64% to 15% using the Curie temperatures reported for Fe–B amorphous alloys.[30] However, the observed values of Curie temperature are lower than those reported for amorphous alloys obtained by melt spinning with similar composition.[30] Several aspects could explain this difference: a Nb enrichment of the amorphous phase with respect to the nominal composition due to the remaining Fe rich nanocrystals and B inclusions and the presence of Cr contamination from milling media [T_C decreases ~25 K/at. % Cr (Ref. 21)]. Moreover, in other two phase materials composed of a ferromagnetic amorphous matrix surrounding ferromagnetic Fe nanocrystals, the Curie temperature of the amorphous phase is enhanced.[31,32] This Curie temperature is shown as a function of equivalent milling time in Fig. 4(d). The predicted Ω^3 law is fulfilled by this parameter, too.

The crystalline fraction dependence of magnetic entropy change at peak temperature, ΔS_M^{pk}, is shown in Fig. 5(a) for both milling processes. It is observed that the ΔS_M^{pk} increases with the amorphous fraction (also appreciated in Fig. 3). This behavior is similar to that observed for partially nanocrystallized melt spun ribbons.[9,18] It can be observed that the increase in ΔS_M^{pk} does not follow a linear trend (the higher the amorphous fraction, the higher the increase in ΔS_M^{pk}) due to

the progressive increases in B content in the matrix. In fact, an increase in boron content has been reported to enhance ΔS_M for Fe–X–B (X=Zr, Mo, etc.) alloys with low B content.[33]

Figure 5(c) shows RC_{FWHM} as a function of crystalline fraction for all studied samples. As amorphous fraction increases a continuous enhancement in the refrigerant capacity is observed. The maximum measured value, for X_C=15%, is higher than that reported for biphasic NiMnGa nanocrystalline powders.[14] Assuming a linear behavior with crystalline fraction, a maximum $RC_{\mathrm{FWHM}} \sim 115$ J kg^{-1} for a maximum applied field of 15 kOe could be extrapolated for a completely amorphous material, which is approximately twice the value that can be estimated from literature results for GdSiGe/Fe ball milled nanopowders.[12] Fitting the refrigerant capacity as a power law of the applied field,[34] a value of the field exponent of ~1.1 is obtained for RC_{FWHM} and ~1.2 for RC_{WP}. Extrapolating to a maximum applied field of 50 kOe and for a completely amorphous material, $RC_{\mathrm{FWHM}} \sim 445$ J kg^{-1} and $RC_{\mathrm{WP}} \sim 283$ J kg^{-1} are obtained. SQUID measurements performed at 5 T are in agreement with these extrapolations. The value obtained for the first method is of the same order as those reported for ball milled Pr_2Fe_{17} alloys.[16] However, the value calculated using the second method is slightly higher than those reported for Pr_2Fe_{17} (Ref. 16) and GdGeSiFe alloys.[35]

The common evolution of the peak magnetic entropy change and refrigerant capacity as a function of equivalent milling time for both milling processes performed at 150 and 350 rpm, respectively [Figs. 5(b) and 5(d)], shows that these two parameters satisfy the Ω^3 scaling law, as it was observed for T_C and magnetization.

The field dependence of the MCE can be expressed as a power law of the field for materials with a second order phase transition: $\Delta S = AH^n$,[36] where A is a prefactor. For single phase materials, the exponent n is 1 for temperatures well below the Curie transition, n=2 well above T_C and $n = 1 + (1/\delta)(1 - 1/\beta)$ at T_C, β and δ being the critical exponents. This behavior was confirmed for different amorphous[36,37] and crystalline alloys.[38,39] Figure 6 shows the temperature dependence of n at a maximum applied magnetic field (15 kOe) for all studied samples. It can be observed that n values at the maximum temperature in the studied range are lower than 2 (value expected for a single phase). In fact, although this temperature, 420 K, is well above the T_C of the amorphous phase, it is well below the expected Curie temperature of the crystalline phase (>1000 K). Therefore, these values of n at 420 K can be explained in terms of the biphasic character of the samples and n would be between the high temperature limit for a paramagnetic phase (n=2) and the low temperature limit for a ferromagnetic phase (n=1).

At Curie transition, whereas for single phase materials $n(T_C)$ is independent of the applied field,[34,36] for multiphase materials n decreases with the applied field.[39,40] Figure 7 shows the temperature dependence of the field exponent for several maximum applied fields for two different volume fractions, confirming the multiphase character of the studied samples. This is also confirmed from the field dependence of

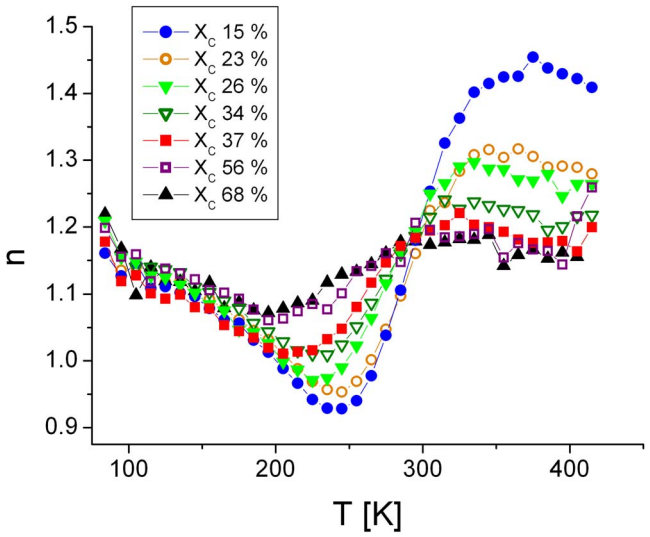

FIG. 6. (Color online) Temperature dependence of the field exponent of ΔS_M for all studied samples and for an applied magnetic field of 15 kOe. Hollow symbols correspond to 150 rpm and solid symbols correspond to 350 rpm.

the change in the depth of the minimum of n, $\Delta n(T_C) = n(T_C, H_2) - n(T_C, H_1)$, where $H_2 < H_1$. The multiphase character of the studied samples is evidenced as $\Delta n(T_C) \neq 0$, i.e., $n(T_C)$ depends on H, unlike the expected behavior for single phase systems, where $\Delta n(T_C) = 0$ as $n(T_C)$ is field independent. In Fig. 7, it is observed that $\Delta n(T_C)$ decreases as X_C decreases, because the studied system becomes closer to a single phase.

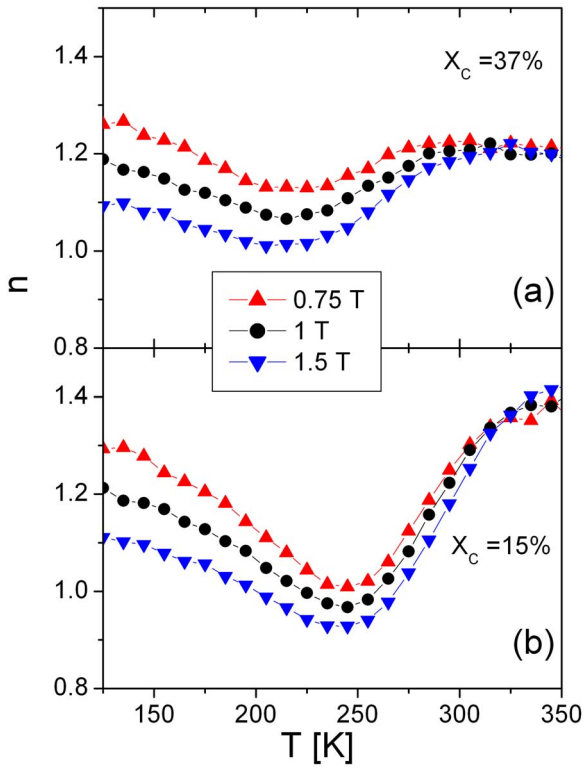

FIG. 7. (Color online) Temperature dependence of the field exponent of ΔS_M for different applied magnetic fields for samples with different crystalline fraction: (a) X_C=37% and (b) X_C=15%. Hollow symbols correspond to 150 rpm and solid symbols correspond to 350 rpm.

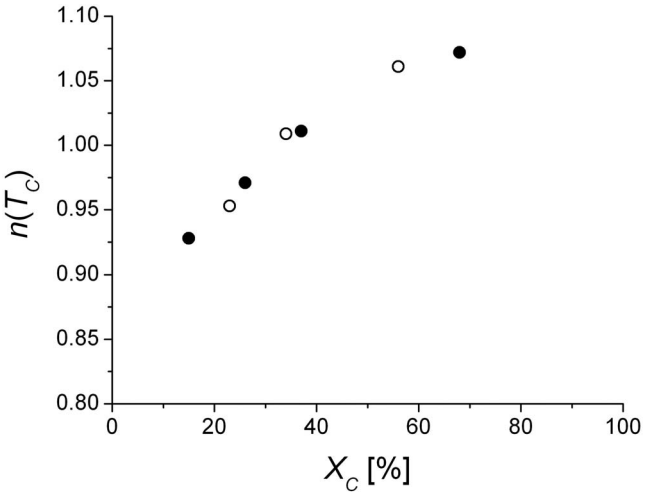

FIG. 8. Field exponent of ΔS_M at Curie temperature as a function of crystalline fraction. Hollow symbols correspond to 150 rpm and solid symbols correspond to 350 rpm.

Figure 8 shows a decrease in $n(T_C)$ as amorphous fraction increases, although higher values than those measured for pure amorphous alloys [~0.75 (Refs. 36 and 37)] are found. This can be explained considering that the total magnetic entropy change of a biphasic system (assuming noninteracting phases) can be expressed as $\Delta S_M^{\mathrm{pk}} = \Delta S^A + \Delta S^C$,[24] where ΔS^A and ΔS^C are the entropy changes at the peak temperature of the amorphous phase for amorphous and crystalline phases, respectively. In this frame and for low amount of the high Curie temperature phase, $n(T_C)$ can be expressed in terms of the field exponents for amorphous, n_A, and crystalline, n_C, phases:[39]

$$n \approx n_A + X_C \frac{c_1}{c_2}(n_C - n_A)H^{n_C - n_A} + \cdots, \tag{2}$$

where c_1 and c_2 are proportionality factors. This expression, for a constant magnetic field, predicts a linear behavior as a function of the amount of the high Curie temperature phase (X_C in the studied case), which should agree with the observed trend in Fig. 8 for $X_C \leq 37\%$. A value of $n(T_C) = 0.86 \pm 0.01$ could be extrapolated for $X_C = 0$. Moreover, a tendency to saturation is observed in Fig. 8 as $X_C = 100\%$ is approached.

V. CONCLUSIONS

The magnetic properties and the magnetocaloric response of the mechanically alloyed $Fe_{75}Nb_{10}B_{15}$ powders were studied for samples with progressive decrease in the crystalline volume fraction down to a minimum value of 15%.

Thermomagnetic properties rescale following a Ω^3 law for different milling processes.

- Curie temperature of the amorphous phase increases as the amorphous fraction increases due to the progressive increase in B content in the amorphous phase.
- The peak magnetic entropy change as well as the refrigerant capacity increase with increasing the amorphous fraction in agreement with the sum rule.
- The multiphase character of the studied samples can explain the anomalies observed for the field dependence of the magnetic entropy change.

ACKNOWLEDGMENTS

This work was supported by the Ministry of Science and Innovation (MICINN) and EU FEDER (Project Nos. MAT2007-65227 and CIT420000-2008-9) and the PAI of the Regional Government of Andalucía (Project No. P06-FQM-01823). J.J.I. acknowledges a fellowship from MICINN. J.S.B. acknowledges a research contract from Junta de Andalucía.

[1] K. A. Gschneidner, Jr. and V. K. Pecharsky, Annu. Rev. Mater. Sci. **30**, 387 (2000).
[2] E. Brück, O. Tegus, D. T. C. Thanh, and K. H. J. Buschow, J. Magn. Magn. Mater. **310**, 2793 (2007).
[3] B. F. Yu, Q. Gao, B. Zhang, X. Z. Meng, and Z. Chen, Int. J. Refrig. **26**, 622 (2003).
[4] V. K. Pecharsky and K. A. Gschneidner, Jr., Phys. Rev. Lett. **78**, 4494 (1997).
[5] V. K. Pecharsky and K. A. Gschneidner, Jr., Appl. Phys. Lett. **70**, 3299 (1997).
[6] W. Choe, V. K. Pecharsky, O. A. Pecharsky, K. A. Gschneidner, Jr., V. G. Young, Jr., and G. J. Miller, Phys. Rev. Lett. **84**, 4617 (2000).
[7] L. Morellon, J. Blasco, P. A. Algarabel, and M. R. Ibarra, Phys. Rev. B **62**, 1022 (2000).
[8] C. B. Zimm, A. Jastrab, A. Sternberg, V. K. Pecharsky, K. A. Gschneidner, Jr., M. Osborne, and I. Anderson, Adv. Cryog. Eng. **43**, 1759 (1998).
[9] V. Franco, J. S. Blázquez, C. F. Conde, and A. Conde, Appl. Phys. Lett. **88**, 042505 (2006).
[10] M. H. Phan and S. C. Yu, Phys. Status Solidi A **204**, 4091 (2007).
[11] E. Brück, O. Tegus, D. T. Cam Thanh, T. Nguyen Trung, and K. H. J. Buschow, Int. J. Refrig. **31**, 763 (2008).
[12] D. M. Rajkumar, M. Manivel Raja, R. Gopalan, and V. Chandrasekaran, J. Magn. Magn. Mater. **320**, 1479 (2008).
[13] J. Gass, H. Srikanth, N. Kislov, S.S. Srinivasan, and Y. Emirov, J. Appl. Phys. **103**, 07B309 (2008).
[14] Y. V. B. de Santanna, M. A. C. de Melo, I. A. Santos, A. A. Coelho, S. Gama, and L. F. Cótica, Solid State Commun. **148**, 289 (2008).
[15] S. Tencé, S. Gorsse, E. Gaudin, and B. Chavalier, Intermetallics **17**, 115 (2009).
[16] P. Gorría, J. L. Sánchez-Lamazares, P. Alvarez, M. J. Pérez, J. Sanchez-Marcos, and J. A. Blanco, J. Phys. D **41**, 192003 (2008).
[17] C. Suryanarayana, Prog. Mater. Sci. **46**, 1 (2001).
[18] I. Skorvanek and J. Kovac, Czech. J. Phys. **54**, 189 (2004).
[19] J. J. Ipus, J. S. Blázquez, V. Franco, and A. Conde, Intermetallics **16**, 1073 (2008).
[20] J. J. Ipus, J. S. Blázquez, V. Franco, M. Millán, A. Conde, D. Oleszak, and T. Kulik, Intermetallics **16**, 470 (2008).
[21] V. Franco, C. F. Conde, and A. Conde, J. Magn. Magn. Mater. **203**, 60 (1999).
[22] J. J. Ipus, J. S. Blázquez, S. Lozano-Perez, and A. Conde, Philos. Mag. **89**, 1415 (2009).
[23] M. E. Wood and W. H. Potter, Cryogenics **25**, 667 (1985).
[24] R. D. McMichael, R. D. Shull, L. J. Swartzendruber, L. H. Bennett, and R. E. Watson, J. Magn. Magn. Mater. **111**, 29 (1992).
[25] H. P. J. Wijn, *Landolt–Börnstein: Magnetische Eigenschaften von Metallen* (Springer, Berlin, 1991), Vol. 19, p. 90.
[26] A. T. Rezende and R. S. Turtelli, IEEE Trans. Magn. **23**, 2128 (1987).
[27] R. M. Bozorth, *Ferromagnetism* (Van Nostrand, Princeton, NJ, 1968), p. 111.
[28] J. M. Barandiaran, P. Gorria, I. Orue, M. L. Fdez-Gubieda, F. Plazaola, and A. Hernando, Phys. Rev. B **54**, 3026 (1996).
[29] M. L. Fdez-Gubieda, A. Garcia-Arribas, J. M. Barandiaran, R. Lopez Anton, I. Orue, P. Gorria, S. Pizzini, and A. Fontaine, Phys. Rev. B **62**, 5746

(2000).
[30]H. P. J. Wijn, *Landolt–Börnstein: Magnetische Eigenschaften von Metallen* (Springer, Berlin, 1991), Vol. 19, pp. 92–94.
[31]A. Hernando and T. Kulik, Phys. Rev. B **49**, 7064 (1994).
[32]A. Hernando, I. Navarro, and P. Gorria, Phys. Rev. B **51**, 3281 (1995).
[33]V. Franco, C. F. Conde, J. S. Blázquez, A. Conde, P. Svec, D. Janickovic, and L. F. Kiss, J. Appl. Phys. **101**, 093903 (2007).
[34]V. Franco, A. Conde, J. M. Romero-Enrique, and J. S. Blázquez, J. Phys.: Condens. Matter **20**, 285207 (2008).
[35]V. Provenzano, A. J. Shapiro, and R. D. Shull, Nature (London) **429**, 853 (2004).
[36]V. Franco, J. S. Blázquez, and A. Conde, Appl. Phys. Lett. **89**, 222512 (2006).
[37]V. Franco, J.S. Blázquez, M. Millán, J.M. Borrego, C.F. Conde, and A. Conde, J. Appl. Phys. **101**, 09C503 (2007).
[38]V. Franco, A. Conde, V. K. Pecharsky, and K. A. Gschneidner, Jr., Europhys. Lett. **79**, 47009 (2007).
[39]V. Franco, R. Caballero-Flores, A. Conde, Q. Y. Dong, and H. W. Zhang, J. Magn. Magn. Mater. **321**, 1115 (2009).
[40]Q. Y. Dong, H. W. Zhang, J. R. Sun, B. G. Shen, and V. Franco, J. Appl. Phys. **103**, 116101 (2008).